Recent increase in species-wide diversity after interspecies introgression in the highly endangered Iberian lynx

Lucena-Perez, Maria; Paijmans, Johanna; Nocete, Francisco ; Nadal, Jordi ; Detry, Cleia ; Dalén, Love; Hofreiter, Michael; Barlow, Axel; Godoy, José

Nature Ecology and Evolution

DOI:
10.1038/s41559-023-02267-7

Published: 15/01/2024

Peer reviewed version

Article

Recent increase in species-wide diversity after interspecies introgression in a highly endangered felid

Maria Lucena-Perez[1],*, Johanna L.A. Paijmans[2,3], Francisco Nocete[4], Jordi Nadal[5], Cleia Detry[6], Love Dalén[7,8], Michael Hofreiter[2], Axel Barlow[9], José A. Godoy[1,*].

[1] Department of Integrative Ecology, Estación Biológica de Doñana, CSIC, C/ Américo Vespucio 26, 41092 Seville, Spain
[2] Evolutionary Adaptive Genomics, University of Potsdam, Karl-Liebknecht-Str. 24-25, 14476 Potsdam, Germany
[3] Department of Zoology, University of Cambridge, Downing Street, Cambridge CB2 3EJ, UK
[4] Grupo de Investigación MIDAS, Departamento Historia I (Prehistoria), Universidad de Huelva, Huelva, Spain
[5] SERP, Departament de Prehistoria, Historia Antiga i Arqueologia, Universitat de Barcelona, Barcelona, Spain
[6] UNIARQ – Centro de Arqueologia da Faculdade de Letras da Universidade de Lisboa, Alameda da Universidade, Lisboa, Portugal
[7] Centre for Palaeogenetics, Svante Arrhenius väg 20C, Stockholm 10691, Sweden
[8] Department of Bioinformatics and Genetics, Swedish Museum of Natural History, Box 50007, Stockholm 10405, Sweden
[9] School of Natural Sciences, Bangor University, Bangor, Gwynedd, LL57 2DG, UK

* Author for correspondence

Abstract

Genetic diversity is lost in small and isolated populations, affecting many globally declining species. Interspecific admixture events can increase genetic variation in the recipient species' gene pool, but empirical examples of species-wide restoration of genetic diversity by admixture are lacking. Here, we present multi-fold coverage genomic data from three ancient Iberian lynx (*Lynx pardinus*) approximately 2-4 thousand years old and show a continuous or recurrent process of interspecies admixture with the Eurasian lynx (*L. lynx*) that increased modern Iberian lynx genetic diversity above that occurring millennia ago despite its recent demographic decline. Our results add to the accumulating evidence for natural admixture and introgression among closely-related species

and show that this can result in an increase of species-wide genetic diversity in highly genetically eroded species. The strict avoidance of interspecific sources in current genetic restoration measures needs to be carefully reconsidered, particularly in cases where no conspecific source population exists.

Introduction

Genetic diversity is an intrinsic and critical component of biodiversity, as it determines adaptive potential and thus influences, together with other genetic and non-genetic factors, the extinction probability of a species under environmental change. However, genetic diversity is being rapidly lost as populations become small and isolated as a consequence of human actions, a process that is often accompanied by increased genetic load, reduced fitness and increased extinction probabilities (Allendorf *et al.* 2021; Frankham *et al.* 2010). It is thus not surprising that the analyses of ancient and historical DNA, which enable past and current diversity to be compared directly, typically find a net loss of genetic diversity through time in declining species and populations (de Bruyn *et al.* 2011; Diez-del-Molino *et al.* 2018; Hofreiter & Barnes 2010; Leigh *et al.* 2019).

Lost genetic diversity can be eventually restored by mutation, but this is a slow process that is also dependent on population size. *De novo* DNA mutation is, however, not the only mechanism by which novel genetic variants can be introduced into a population's gene pool. Gene flow from other conspecific populations can reintroduce lost variation and slow down or even reverse diversity loss, and reinforcement of gene flow has proved an effective management strategy to restore diversity and, eventually, fitness and adaptive potential (Ralls *et al.* 2018). As for interspecific gene flow, the situation is less straightforward because the species is generally regarded as a closed system, so that the potential for restoration by hybridization is often negated. However, it is now widely recognized that the occurrence of admixture between species is much more common than previously thought. Particularly for mammals, a spate of recent genomic studies has uncovered widespread admixture within several major clades, involving both extant and extinct species (Barlow *et al.* 2018; Iacolina *et al.* 2019; Kumar *et al.* 2017; Li *et al.* 2016; Palkopoulou *et al.* 2018). These interspecific admixture events will increase genetic variation in the recipient species' gene pool, which may persist and become widespread across the species populations. Thus, it is possible, at least in theory, for interspecies admixture to reverse the genetic loss caused by recent population size declines, although its use as a restoration measure is generally discouraged due to the risk of outbreeding depression and the loss of species "identity" (Chan et al. 2019; Quilodrán et al. 2020).

The Iberian lynx (*Lynx pardinus*) is one of the four species in the genus *Lynx*, which also includes the bobcat (*L. rufus*), the Canada lynx (*L. canadensis*) and the Eurasian lynx (*L. lynx*). Eurasian and Iberian lynx were once separated only at the subspecies level (Corbet & Hill 1986; Tumlison 1987; Weigel 1961), although their coexistence in Southern Europe during most of the Pleistocene and the absence of intermediate forms support their recognition as distinct species (Brink 1970; Kurten & Granqvist 1987; Matjuschkin 1978; Werdelin 1981). The most common phylogeny across autosomal windows, and thus the consensus autosomal phylogeny, place the Iberian and the Eurasian lynx as sister species diverging around 1.0 Mya; however, low recombination regions in autosomes, and particularly in the X chromosome, supports an alternative tree where Eurasian and Canada lynx are sister species, with Iberian lynx diverging earlier (around 1.5 Mya; Li *et al.* 2019, Harris, *et al.* 2022). These contrasting patterns indicate extensive introgression between the Eurasian and Iberian lynx distorting the divergence history in high recombination regions of the genome (Li *et al.* 2019). The Iberian lynx experienced a severe population bottleneck during the 20th century, which resulted in two small and isolated populations by the end of the century (Casas-Marcé *et al.* 2017). Genome-wide studies have shown that current Iberian lynx genetic diversity is among the lowest recorded for any mammal (Abascal *et al.* 2016), and the comparison of microsatellite data of historical Iberian lynx and mitogenomic data of historical and ancient samples with that of modern samples revealed a decline in genetic diversity associated with the recent bottleneck (Casas-Marcé *et al.* 2017). However, ancient nuclear genetic data that would allow this recent decline to be placed within the broader context of Iberian lynx evolution is currently lacking. In this study, we generate palaeogenomic data from ancient Iberian lynx dated ~2–4 thousand years ago (kya). We find ancient lynx to exhibit even lower genetic diversity than their modern conspecifics, which can be explained by a recent pulse of admixture with the closely-related Eurasian lynx (*L. lynx*).

Results

Genome sequencing of ancient Iberian lynx

We generated palaeogenomic data from three Iberian lynx samples previously investigated for mitochondrial DNA (Casas-Marcé *et al.* 2017) from Eras del Alcázar, Andújar, Spain (4,270 ± 30 years before present (BP)), La Moleta del Remei, Alcanar, Catalonia, Spain (2,520 ± 30 BP), and Monte Molião, Algarve, Portugal (dated by archeological context approximately 2,070 BP) (Fig. 1A, Table S1). Sample bone powder was pre-treated with sodium hypochlorite to reduce contamination (Korlević *et al.* 2015). Approximately 400–900 million sequences were then generated from each sample using Illumina sequencing, and mapped to the reference genome

assemblies of the Iberian lynx and the domestic cat. This provided a depth of genome coverage of 2.3x (Algarve), 4.3x (Catalonia) and 2.5x (Andújar), and 1.8x (Algarve), 3.5x (Catalonia), and 2.0x (Andújar), when mapped to the Iberian lynx and the domestic cat reference genomes, respectively. All samples show typical ancient DNA damage patterns of C→T substitutions at the fragment ends (Fig. S1). Two of the ancient lynx were males (Catalonia and Andújar) and one was a female (Algarve).

Genomic data from modern Eurasian lynx (Bazzicalupo *et al.* 2022; Lucena-Perez *et al.* 2020), and from an ancient (2,570 ± 30 BP) Eurasian lynx from the north of the Iberian Peninsula (Sima de Pagolusieta in Vizcaya, Spain; Lucena-Perez *et al.* 2022) were included in our study for comparative purposes. Our final dataset comprised 30 modern Iberian lynx from the two remaining populations, Andújar (n=18) and Doñana (n=12) (Kleinman-Ruiz *et al.* 2022; Lucena-Perez *et al.* 2021), and 12 Eurasian lynx from six different populations distributed along an east-west gradient (Balkans, Carpathians, Kirov, Caucasus, Yakutia and Primorsky Krai; n=2 for each population). Sample and sequencing details, including depth of coverage, can be seen in Tables S2 and S3, respectively.

Population structure of Iberian lynx

Previous studies have shown that the two surviving Iberian lynx populations show a high degree of genetic differentiation (Casas-Marcé *et al.* 2017). Microsatellite data from historical populations across their former distribution have shown a lower overall degree of genetic structure in historical times, and modern Andújar being less differentiated from other historical populations than the more isolated modern Doñana population, consistent with Andújar maintaining larger population sizes and higher connectivity until very recently (Casas-Marcé *et al.* 2017). Our novel genome-based results show a relative homogeneity of the ancient Iberian lynx, when analysed together with Andújar and Doñana contemporary populations, in both PCA and individual-based clustering analyses (Fig. 1B-C). The ancient Iberian lynx are also closer to the Andújar population than to the Doñana population, both in the PCA and the individual-based clustering analysis when two *a priori* subpopulations are specified (K=2) (Fig. 1B-C). When specifying K=3, the ancient populations emerge as a separate cluster, with varying degrees of shared ancestry with the Andújar population depending on the run considered (Fig. 1C). However, we observe that PC3 of the PCA separates the ancient Catalonian individual from the other Iberian lynx (Fig. 1B), suggesting the occurrence of some geographical or temporal structure. This ancient structure is, in any case, shallower than that observed between the two surviving populations, and shallower than potential substructuring within the Andújar population, as shown by the dispersion of contemporary Andújar samples in PC2 and

PC3, and subsequent partitions on the individual clustering analysis, which split the contemporary Andújar population at K=4 and the Doñana population at K=5, but maintain the ancient populations as a single cluster (Fig. S2).

Genetic diversity of Iberian lynx

We compared the genetic diversity of modern and ancient Iberian lynx using both individual variables (i.e., observed autosomal heterozygosity), and population variables (i.e., nucleotide diversity, π, and Watterson estimator, θ_W). Unexpectedly, the genetic diversity of ancient lynxes is lower than that of contemporary lynxes, as reflected in observed individual heterozygosity (Fig. 1D, Table S4) and population diversity measures, both π and θ_W (Fig. S3, Table S5). For instance, θ_W diversity in the ancient population (θ_W Ancient=9.50 e-06) represents ~62%, and ~38% of θ_W in Doñana and Andújar, respectively (Fig. S3, Table S5).

The observed pattern is opposite to that expected from artefacts associated to the use of ancient degraded materials, where sequencing errors and post-mortem damage are expected to artefactually increase genetic diversity, and is robust to changes in reference genome, mapping algorithms and to the inclusion/exclusion of transitions (Fig. S3, Table S5). Lower diversity in ancient samples also does not seem to be caused by differences in depth of sequencing coverage, as contemporary samples were subsampled to a depth of coverage similar to the one shown by ancient samples (~2.5x), for both individual and population diversity measures (see methods). We nevertheless investigated the potential relationship between observed heterozygosity and depth of coverage further by using linear regression (Fig. 1D). Although a positive correlation between observed heterozygosity and depth of coverage is observed, the heterozygosities of subsampled modern genomes are consistently higher than those of ancient samples (Fig. 1D), and their ranges do not overlap after the ancient sample of Catalonia (highest ancient depth of 4.3x) is subsampled to a comparable depth of 2.58x, resulting in an observed heterozygosity of 3.15 e-6. This rejects sequencing depth as the sole factor driving differences in observed heterozygosity.

Differences in population genomic diversity between ancient and modern Iberian lynx are consistent across different genomic categories such as promoters, UTR regions, coding sequences, introns or small RNAs (Fig. 2A). Relative genetic diversity differences were however consistently lower in CDS than in intergenic or intron regions (Fig S4), and genome regions showing the largest diversity differences between ancient and modern Iberian lynx show no evidence of enrichment for coding regions (Fig. 2B), suggesting that the difference in diversity is not related to the relaxation of purifying selection in contemporary lynx.

Admixture with Eurasian lynx

The increase in genetic diversity observed in modern relative to ancient Iberian lynx is incompatible with a demographic history of major population declines and extirpation over most of their historical range in the last few centuries. Nor is it easily explained by an inadvertent sampling of three isolated and low diversity ancient populations, since population analyses suggest low levels of ancient genetic structure and a close affinity of the three ancient Iberian lynx to the Andújar population. We therefore tested a hypothesis of interspecies admixture in the intervening time period between the ancient and modern Iberian lynx as a potential source of novel genetic variation leading to an increase in diversity.

D statistic tests showed that all modern Iberian lynx share a significant excess of derived alleles with their sister species, the Eurasian lynx (*L. lynx*), relative to all ancient Iberian lynx, consistent with gene flow between Eurasian lynx and Iberian lynx in the last 2 ka (Fig. 3A). We also find varying levels of admixture with Eurasian lynx occur among the ancient Iberian lynx individuals in a gradient in which more recent individuals show more derived alleles with Eurasian lynx (Fig. 3B, 3C, 3D). Precisely, the more recent ancient individuals from Catalonia (2.5 kya) and Algarve (2 kya) share similar derived alleles with Eurasian lynx (Fig. 3B), while the oldest individual from Andújar (4.2 ka) share fewer derived alleles with Eurasian lynx than those two (Fig. 3C, 3D). Gene flow from Eurasian lynx has permeated the entire modern Iberian lynx distribution, as the proportion of admixed alleles in modern individuals is similar in the two surviving populations (Fig. S5A).

As for the donor population, we find that western Eurasian individuals share an excess of derived alleles with contemporary Iberian lynx relative to Eurasian lynx from Asia (Fig. 3E), whereas there is a relative homogeneity in interspecies admixture levels among different western or different eastern populations (Fig. S5B, S5C).To further investigate the timing and geographic source of admixture we used an ancient Eurasian lynx that inhabited the Iberian Peninsula 2 kya (Lucena-Perez *et al.* 2022). Contemporary Iberian lynx share more alleles with contemporary Eurasian lynx from both eastern and western populations than with the ancient Eurasian lynx inhabiting the Iberian Peninsula (Fig. S5D, S5E). Also, the ancient Iberian lynx do show evidence of admixture with contemporary Eurasian lynx, but less than with the ancient Eurasian lynx from Iberia: they share more alleles with western contemporary individuals than with the ancient Eurasian lynx, the amounts shared with the latter being similar to those shared with the eastern contemporary populations (Fig. S5F, S5G).

Directional gene flow from Eurasian lynx into Iberian lynx

D statistics do not allow the direction of gene flow to be identified. To investigate this, we used an approach developed for low coverage palaeogenomes that examines the occurrence of phylogenies compatible with admixture along non-overlapping genomic blocks (Barlow *et al.* 2018). The test involves two individuals of each admixing species that vary in their amount of admixture. We test the hypothesis that a species is the donor or the recipient of gene flow by comparing the frequency of genome blocks where the more admixed individual groups with the opposing species' clade, relative to the frequency where the less admixed individual groups with the opposing species' clade. An increase in the former provides evidence that the species is the recipient of gene flow. We selected the highest coverage ancient Iberian lynx (Catalonia, 2,520 ± 30 BP, 3.5x when mapped to the domestic cat reference) for these tests, which were repeated using all modern Iberian lynx individuals. For Eurasian lynx we used an individual from the Balkans and one from Yakutia to represent the two major Eurasian lynx clades. In particular, we examined for an increase in the number of genomic blocks where the more-admixed modern Iberian lynx groups with Eurasian lynx (with the less-admixed ancient Iberian lynx in a basal position), relative to the opposite pattern, with the less-admixed ancient Iberian lynx grouping with Eurasian lynx (and the more-admixed modern Iberian lynx in a basal position). For all modern Iberian lynx, we found that genomic blocks where the more-admixed modern Iberian lynx groups with Eurasian lynx outnumber the opposite pattern by a factor of 1.4–2.6 (Fig. S6). Although we do not rule out bidirectional gene flow, these results indicate that the identified admixture event(s) between the two species transferred alleles from Eurasian lynx into Iberian lynx, consistent with the observed increase in genetic diversity.

Quantifying admixture fractions in modern Iberian lynx

Having verified the occurrence of directional gene flow from Eurasian into Iberian lynx, we estimated the admixed fraction of the genomes of modern Iberian lynx relative to ancient Iberian lynx using the $\hat{f}$ statistic.$\hat{f}$ assumes unidirectional admixture between donor and recipient species, and will tend to underestimate the admixed fraction if gene flow was bidirectional, and is thus a conservative measure. The estimated admixture fractions are remarkably consistent among modern Iberian lynx irrespective of the western Eurasian lynx individuals used in the comparisons (Fig. 4). Consistent variation is also observed when different ancient Iberian lynx are used, leading to an estimated excess admixture in modern Iberian lynx of around 2% when compared to the ancient individuals from Catalonia (2.5 kya) and Andujar (4.2 kya), and around 1.2% when compared to the more recent individual from Algarve (2 kya).

Discussion

A general trend of reduced genetic diversity in current compared to ancient populations is well documented among species that have undergone postglacial or historical population declines where ancient or historical diversity are directly compared to current diversity (D'Elia *et al.* 2016; Dufresnes *et al.* 2018; Dussex *et al.* 2018; Feng *et al.* 2019; Sánchez-Barreiro *et al.* 2021; Sheng *et al.* 2018; van der Valk *et al.* 2019). The Iberian lynx is one good example of species that lost significant amounts of both mitochondrial and nuclear genetic diversity following a process of steep decline, fragmentation and local extirpation in the 20th century (Casas-Marcé *et al.* 2017). Recent genetic erosion, evidence of other serial bottlenecks and low effective sizes throughout most of the species' history have been invoked to explain the extremely low genome-wide and species-wide genetic diversity of Iberian lynx (Abascal *et al.* 2016). Here, we report the unexpected observation of two to three-times lower genomic diversity in ancient (2,000-4,000 ya) than in contemporary Iberian lynx individuals, and postulate admixture with its sister species, the Eurasian lynx, as the most likely cause of the observed increase. Although similar processes have been reported following intraspecific gene flow in small isolated populations (Vila et al. 2003), here we demonstrate an increase in genetic diversity across an entire species following an event of gene flow from a closely-related species.

Genomic evidence for extensive admixture between Eurasian and Iberian lynxes since their divergence is abundant and comes from phylogenomic, D-statistics and model-based approaches (Abascal *et al.* 2016; Li *et al.* 2016; Li *et al.* 2019). Although the two species show non-overlapping disjunct distributions now, this was not the case in the past. The Iberian lynx extended its range during the late Pleistocene and early Holocene into Southern France and northern and, possibly, southern Italy, where it likely coexisted with the Eurasian lynx, and the Eurasian lynx inhabited the north of the Iberian Peninsula until the early 20th century (Clavero & Delibes 2013; Jiménez *et al.* 2018; Mecozzi *et al.* 2021; Rodríguez-Varela *et al.* 2016; Rodríguez-Varela *et al.* 2015). Opportunities for encounter and thus hybridization did indeed occur in historical times in Iberia, although direct genetic evidence for this has been absent until now.

Our results provide this lacking evidence and some indication on the timing and geographic patterns of previous admixture events. First, ancient Iberian lynx from Catalonia (2.5 kya), and Algarve (2 kya) were already admixed with Eurasian lynx, although to a lesser extent than contemporary lynxes; and our oldest ancient Iberian lynx (Andújar, 4.2 kya) showed less introgression than younger ancient lynxes (Catalonia, 2.5 kya, and Algarve, 2 kya), suggesting a continuous or

recurrent process rather than a sporadic event. Secondly, consistent with geography, western Eurasian lynx have contributed more alleles to the Iberian lynx genome than the eastern lineage; however, some signal of introgression is present from eastern lynx. This may not be surprising given eastern and western Eurasian lineages started to diverge around 100 kya and gene flow was maintained until 22–15 kya (Bazzicalupo *et al.* 2022; Lucena-Perez *et al.* 2020). Signals of introgression from eastern Eurasian lynx may thus be attributed to admixture events occurring before this divergence and to a high proportion of derived alleles being shared across eastern and western populations from their ancestral population. Thirdly, we found no major differences in introgression levels across contemporary populations of western Eurasian or Iberian lynx, indicating that introgression predated the differentiation of current populations, which has been estimated to have occurred 200 years ago for Iberian lynx, and during the Holocene, with a drastic intensification in historical times due to drift, for Eurasian lynx populations in western Europe (Casas-Marcé *et al.* 2017; Lucena-Perez *et al.* 2020). Surprisingly, though, the single ancient genome of Eurasian lynx from Iberia showed less evidence of admixture with Iberian lynx than other contemporary western lynx populations, indicating that the main source of introgression during the last few millennia may have been a differentiated ancestral population more closely related to contemporary western populations. A more extensive sampling of ancient Eurasian and Iberian lynx genomes may further elucidate the geographic and temporal patterns of admixture between these two species.

The concurrence of patterns of higher autosomal diversity and higher introgression in contemporary compared to ancient Iberian lynx individuals supports the hypothesis that the former is the consequence of the latter. We nevertheless tested the possibility that increased genetic diversity is due to the accumulation of mildly deleterious variation caused by the relaxation of purifying selection during the species' decline. However, increased diversity in modern Iberian lynx is observed in both constrained (e. g. coding) and supposedly neutral (e.g. intergenic) sequences. Both an overall smaller relative increase in CDS, and the lack of enrichment of coding regions among windows with largest diversity increases discard the relaxation of purifying selection as the sole cause of the observed differences. Finally, although the estimated amount of differential introgression may seem small to produce such a large proportional increase in diversity, it must be noted that with an observed rate of divergence between modern Eurasian and Iberian lynx of 1.19 fixed differences per kilobase, a 2% introgression would introduce ca. 60,000 new variants, almost ten times the number of heterozygous positions observed in ancient samples. Future studies will further assess the relationship between local introgression and heterozygosity along the genome.

Beyond providing insights on the evolutionary history of the Iberian lynx, one of the world's rarest cat species, our results are also of wider interest for the conservation of species, particularly in the context of genetic rescue. This widely debated and sometimes controversial conservation strategy involves the introduction of distantly related individuals into imperiled and genetically depauperate populations to restore their fitness and evolutionary potential (Bell *et al.* 2019; Tallmon *et al.* 2004; Whiteley *et al.* 2015). The use of closely related species for genetic rescue is generally discouraged due to presumed risks of outbreeding depression caused by either intrinsic or extrinsic incompatibilities. Nonetheless, our results add to the accumulating evidence for natural admixture and introgression in the genomes of many species and they show that this can result in a substantial increase in the standing genetic diversity in highly eroded populations. The strict avoidance of interspecific sources in genetic restoration measures may need to be carefully reconsidered, particularly in cases like the Iberian lynx where no additional conspecific source population exists, so a closely related species might be the only source of novel genetic diversity.

Methods

Samples

Ancient DNA data was obtained from Iberian lynx archeological and paleontological remains. We tested 20 ancient samples selected based on their sequencing performance among the 58 samples analyzed in Casas-Marcé *et al.* (2017). Three of them yielded enough genomic data for further analyses, and are the main subjects of this study (Table S1). Data from modern samples was obtained from (Lucena-Perez *et al.* 2021; Lucena-Perez *et al.* 2020) and data for the ancient Eurasian lynx sample was obtained from Lucena-Perez *et al.* (2022) (Table S2).

Laboratory methods

All laboratory work was carried out in dedicated ancient DNA facilities at the University of Potsdam, following established procedures to prevent contamination with modern or synthetic DNA (Fulton 2012). We performed 70 DNA extractions from 20 archaeological samples, selected based on mitogenome sequence yield (Casas-Marcé *et al.* 2017). Negative controls were included in all experiments. We drilled the remains to get a variable amount of bone powder up to a maximum of

50 mg. For Algarve and Catalonia sample extraction, we pre-treated the samples with 1 ml 0.5% bleach for 15 min at room temperature to minimize DNA contamination (Korlević *et al.* 2015). For all three ancient samples, bone powder was then digested for ~18 h at 37°C in 1 ml extraction buffer (0.45 M EDTA, 0.25 mg/ml Proteinase K) with constant rotation. DNA in the resulting supernatant was purified following the protocol by (Dabney et al. 2013), which maximizes degraded DNA recovery by increasing the ratio of binding buffer to sample (13:1).

DNA extracts were converted into sequencing libraries using the single-stranded protocol described in Gansauge and Meyer (2013). Prior to library preparation DNA extracts were treated with UDG (uracil-DNA glycosylase) and endonuclease VIII to remove deoxyuracils resulting from postmortem DNA damage. Then double-stranded DNA was denatured and a biotinylated adapter oligo was ligated to the 3'end of each molecule. Resulting products were immobilized on Streptavidin-coated beads to repair blunt ends, and the P5 adapter was ligated to the template molecule. We performed a qPCR to evaluate library concentration and used this information to estimate the minimal number of amplification cycles to use in the indexing PCR to avoid clonality (Ancient Andujar: 6 cycles; Ancient Algarve: 8 cycles; Ancient Catalonia: 9 cycles). Indexing of single-stranded libraries incorporated an index sequence next to the P7 and P5 adapters using PCR with AccuPrime Pfx DNA polymerase (ThermoFisher) for its ability to read over uracil (Dabney & Meyer 2012). Indexed libraries were quantified using Qubit 2.0 fluorometer (ThermoFisher Scientific) and 2200 TapeStation Instrument, and pooled in an equimolar ratio.

A test sequencing to evaluate endogenous content was done using the Illumina MiSeq sequencing platform, producing 2x70pb paired-end (PE) reads. Out of the 70 libraries prepared, 4 libraries, coming from 3 samples (Fig. 1A), showed an endogenous content above 10%. These libraries were checked for complexity using Preseq software (http://smithlabresearch.org/software/preseq/), before

major sequencing using the Illumina HiSeq X sequencing platform (2x 150 bp paired-end reads) in the Swedish Museum of Natural History.

Data processing

Contemporary and ancient data were processed following the same pipeline. Whole genome re-sequencing data was quality-checked using FastQC (https://www.bioinformatics.babraham.ac.uk/projects/fastqc). Overlapping reads were merged, and adapters and low quality reads removed, using SeqPrep (https://github.com/jstjohn/SeqPrep), with default parameters with reads shorter than 30 bp removed. Merged reads coming from ancient samples, and merged and unmerged contemporary data were mapped to the 2.8 Gb *Lynx pardinus* genome (Abascal *et al.* 2016), and the 2.5Gb *Felis catus* genome v9.0 (GCF_000181335.3) (Buckley *et al.* 2020) using bwa aln 7.17 (Li & Durbin 2009). After removing reads with mapping quality below 30 and sorting using samtools (Li et al. 2009), we added read groups (https://broadinstitute.github.io/picard), merged sequencing runs on an individual basis (Li et al. 2009), marked duplicates using picard-tools (https://broadinstitute.github.io/picard), and realigned using GATK (McKenna *et al.* 2010). Coverage, mapping statistics, and read length distributions were calculated using samtools (Li et al. 2009). The authenticity of the ancient data was checked by the small fragment length distribution, and the existence of ancient DNA damage -excess of C to T substitutions at the ends of the reads-, as revealed by mapDamage (Jónsson *et al.* 2013) (Fig. S1). Mapping to Iberian lynx reference genome was used for structure and diversity analysis, while mapping to the domestic cat reference genome was used for d-stat tests to avoid previously reported reference bias (Sheng et al. 2019). For all our analysis we excluded the previously identified low complexity and low mappability regions in lynx or in cat, as well as X and Y chromosome when specified (Abascal *et al.* 2016; Buckley *et al.* 2020). We also sexed the samples by calculating the ratio of depth of coverage on the X chromosome to that of the A1 autosome. This method was validated using contemporary samples of known sex.

To avoid depth of coverage bias we subsampled our contemporary Iberian lynx mapped samples to a depth of coverage similar to the ancient samples (~2.5x) using samtools (Li et al. 2009), and used these subsampled datasets for population structure analysis (PCA and clustering) and genetic diversity analysis. For admixture analysis (D-statistics, gene flow direction test and $\hat{f}$ analysis) we used pseudo-haplodized data (details in each section). Percentage of duplicated reads, original and subsampled depth of coverage, when it applies, are shown in Table S3.

Population structure

Principal component analysis (PCA) was done for contemporary Iberian lynx data using ANGSD. We calculated the genotype posterior probabilities using ANGSD (Kim et al. 2011; Li 2011) and NGSTools/ngsPopGen/ngsCovar (Fumagalli 2013; Fumagalli *et al.* 2014) with the following filters (-uniqueOnly 1 -remove_bads 1 -only_proper_pairs 1 -baq 1 -C 50 -minMapQ 30 -minQ 20 -doCounts 1 –minInd (number of individuals in the population/2) –setMaxDepth (3*sqrt(average (AVR) depth for the population)) -skipTriallelic 1 –SNP_pval 1e-3. To infer the ancestral state we used a fasta sequence of *L. rufus* covering 97% of our bases obtained after mapping reads to the Iberian lynx genome, calling variants using SAMtools mpileup (-q 30) (Li et al. 2009), and pseudohaploidizing using pu2fa (-C45) (https://github.com/Paleogenomics/Chrom-Compare). As heterogeneity along the genome in depth of coverage in the ancient samples can artificially distort PCA axes, , we performed four different PCA: one including only contemporary data, and three PCA including contemporary samples plus one different ancient sample each. Then we projected each individual ancient PCA, i.e. the coordinates of contemporary and ancient samples obtained in each of the PCA including one ancient individual, onto the axes obtained in the PCA using only contemporary data. We did that using Procrustes analysis, following Borg and Groenen (1997), and using the package MCMCpack (Martin *et al.* 2011) in R (R_Core_Team 2019). This produced new transformed coordinates for the contemporary individuals. After repeating the procedure for all

three PCA including an ancient sample, we, finally, plotted the mean of all the transformed and the original contemporary coordinates, plus the ancient coordinates, together.

Genotype likelihoods calculated with ANGSD (Kim et al. 2011; Li 2011) were used for a genomic clustering analysis using NGSadmix (Li 2011; Skotte *et al.* 2013) with the same filters used for PCA analysis. NGSadmix was run 10 times from K=1 to K=5, and the results were plotted using R. Optimal K was evaluated following (Evanno *et al.* 2005), using CLUMPAK (Kopelman *et al.* 2015).

Nuclear genomic diversity

We calculated individual heterozygosity using ANGSD (Korneliussen *et al.* 2014; Korneliussen *et al.* 2013; Li 2011), and realSFS (Korneliussen *et al.* 2013) in an individual-by-individual basis. Individual heterozygosity is the second value of the SFS when calculated for a diploid individual. We explored the relationship between diversity and depth of coverage by plotting the correlation between heterozygosity and depth.

At a population level, two measures of genetic diversity per site (nucleotide diversity (π), and Watterson's estimator (θ_W)) were calculated using ANGSD (Korneliussen *et al.* 2014; Korneliussen *et al.* 2013; Li 2011), and realSFS (Korneliussen *et al.* 2013). The analysis was ran for 5 different groups of 3 random individuals in the contemporary populations. Using thetaStat (Korneliussen *et al.* 2013), we performed a sliding-window approach with a window size set to 50,000 bp and a step size of 10,000. All filters described for PCA were also used for diversity calculation except –SNP_pval (not applicable). We calculated mean diversity weighted by the number of informative sites in each window, and standard deviation by bootstrapping over windows as implemented in the *boot* package for R (Canty & Ripley 2014), to account for correlation among nearby sites due to

linkage disequilibrium (LD). Finally, we computed the average of all iterations for the contemporary populations and calculated the standard deviation.

To check whether diversity differences were conspicuous along the genome we calculated average diversity (π, and θ_W) using ANGSD (Korneliussen *et al.* 2014; Korneliussen *et al.* 2013; Li 2011), and realSFS (Korneliussen *et al.* 2013) across different genomic features representing neutral vs. evolutionary constrained regions, namely intergenic regions, coding gene promoters, 5' untranslated regions (UTR), coding sequence (CDS), introns, 3' untranslated regions (UTR), long-non-coding (lnc) RNA promoters, lnc RNA exons, lnc RNA introns, non-coding (nc) RNA (mostly miRNAs, snRNAs and snoRNAs), and ultra-conserved-non-coding-elements (UCNE), for the ancient and the contemporary populations. To do so, we concatenated positions of the genomic feature considered and did a window based analysis with window size equal 10kb and window step 5kb. To avoid biases due to differences in sample size, we randomly selected one of the five contemporary iterations of size n=3 for this analysis. Standard deviation was calculated using a bootstrapping over windows procedure implemented in the R package *boot* (Canty & Ripley 2014) with 100 iterations. Relative difference between overall ancient and contemporary genetic diversity in different features was calculated as in Lucena-Perez et al. (2021). We further tested whether topological widows with largest differences in diversity (π, and θ_W) in contemporary versus ancient comparisons were enriched or depleted in CDS sites. To do so, we calculated differences in diversity between the ancient and the contemporary population by windows and calculated mean and standard deviation of the difference distribution. Diversity outlier windows were defined as windows with a difference in diversity lower than (typically negative) value of the mean - 2*standard deviation. Then, we calculated the percentage of CDS sites for each window, and compared the distribution and mean of CDS percentage in outliers *vs.* non-outlier windows.

Admixture between species

We tested for admixture between Iberian lynx and Eurasian lynx populations with the D statistic (Durand *et al.* 2011; Green *et al.* 2010), using the data mapped to the domestic cat genome to avoid reference bias (Barlow *et al.* 2018; Gunther & Nettelblad 2019). This method uses haploidized sequences of 4 individuals representing: two sister populations (P1 and P2), a potential introgressing population (P3), and an outgroup (P4) to define ancestral alleles (A). Then, it identifies how many derived alleles (B) are shared between P1 and P3, and between P2 and P3, leading to two different patterns: ABBA – derived allele shared by P2 and P3; and BABA – derived allele shared between P1 and P3. The D statistics then is calculated as [sum(ABBA) – sum(BABA)] / [sum(ABBA) + sum(BABA)]. Under incomplete lineage sorting we expect that ABBA occurred at the same frequency as BABA and hence, the D value would be 0. Excess of ABBA or BABA results in positive or negative non-zero D values, and are interpreted as admixture between P2-P3 and between P1-P3, respectively.

The standard practice for generating pseudohaploid sequences for D statistic analysis of palaeogenome data has been to identify alleles by randomly selecting a single read from the read stack, to overcome any differences in sequencing coverage. However, this can be problematic when the ancient dataset is in P1 or P2, because excessive errors cause derived alleles that define the ingroup (BBBA) to be converted into D statistic informative sites (Barlow *et al.* 2020). We therefore used the Consensify method, which calls a majority consensus from a random sample of three reads, to generate haploidised sequences (Barlow *et al.* 2020). This method greatly reduces the error rate of the inferred alleles, while maintaining the reduction of coverage bias provided by single read sampling, and hence reduces the rate of false positives in D statistic analysis

We carried out allele counts for each dataset in ANGSD, with map and base quality filters applied (-minMapQ 30, -minQ 30). Consensify (https://github.com/jlapaijmans/Consensify) was run on the resulting output files specifying a maximum depth filter of the integer read number below the 95th percentile of coverage, calculated in advance using ANGSD. We then tested for admixture on

topologies compatible with the sister group relationship of Iberian and Eurasian lynx, as indicated in Figure 3, using the program D_stat.cpp and the python script D-stat_parser.py, available at https://github.com/jacahill/Admixture. The domestic cat (*Felis catus*) was used as outgroup. Significance was assessed using a weighted block jack-knife based on 5 megabase genome windows, with absolute Z-scores > 3 being considered statistically supported (Durand *et al.* 2011).

Phylogenetic test of gene flow direction

The D statistic does not provide an explicit test of the direction(s) of gene flow. In order to test the donor and recipient relationship in the identified admixture between Eurasian and Iberian lynx, we applied a method based on the observed frequencies of opposing tree topologies along a set of 100 kb non-overlapping windows. This method is described in Barlow et al. (2018), and is conceptually identical to the test of gene flow direction provided by DFOIL statistics (Pease et al. 2015), except that it uses counts of phylogenetic tree topologies, as opposed to SNPs, which have been shown to be more robust to distortion by high error rates typical of palaeogenomic datasets (Barlow et al. 2020). It analyses four individuals with a symmetrical species tree: ((Iberian+, Iberian-),(Eurasian+, Eurasian-)), with +/- denoting individuals that are more/less admixed, as identified by prior D statistics analysis. In this experimental design, if the variability in admixture among the Iberian individuals is explained by gene flow from Eurasian into Iberian lynx, this will cause an excess of non-symmetrical tree topologies with Iberian- in the basal position, relative to the number with Iberian+ in the basal position. To maximise sensitivity, the analysis was carried out for each contemporary Iberian lynx, using representative individuals of ancient Iberian lynx and contemporary Eurasian lynx selected to maximise the observed D values and the level of sequencing coverage. Pseudohaploid sequences were generated using random single-read sampling in angsd, with base (-minQ 30) and map (-minMapQ 30) quality filters applied. A custom bash script making use of the SNP-sites program (Page *et al.* 2016) was then used to divide the aligned sequences into 100 kb non-overlapping windows, and to calculate the maximum-likelihood

phylogeny of each using the BINGAMMA model in RaxML (Stamatakis 2006), and the domestic cat as outgroup to root the trees.

$\hat{f}$ analysis

After determining the predominant direction of gene flow was from Eurasian into Iberian lynx, we estimated the introgressed genome fraction in contemporary Iberian lynx above that occuring in ancient Iberian lynx assuming unidirectional gene flow using the $\hat{f}$ method (Durand *et al.* 2011). The $\hat{f}$ statistics measures the excess of shared derived alleles between the admixed individual and candidate introgressor standardized by the maximum excess of shared derived alleles expected in an entirely (100%) introgressed individual. These analyses used the same Consensify sequences as used in D statistic analysis, and the F_hat.cpp program and the python script F_hat_parser.py (available at https://github.com/jacahill/Admixture). We ran these tests using all combinations of contemporary and ancient Iberian lynx, and western Eurasian lynx. The latter were selected as best representing the introgressing Eurasian lynx population, which likely occurred at the contact zone between the two species in western Europe. Outgroup and tests of significance were as described for the D statistics analyses.

Figures

Fig. 1. A. Contemporary and ancient sampling, with the number of individuals sampled in parenthesis. Ancient Iberian lynx distribution is shown in grey and contemporary (around year 2002, following the decline of the 20th century and previous to any translocation and reintroduction) distribution is shown in black. B. Principal component analysis. Plots of PC1-PC2, and PC2–PC3 are shown, including the percentage of the variance explained by each axis (in parenthesis). C. Relationships among individuals based on individual-based clustering. Results are

shown for K=2 and K=3. For K=2 all runs converge to the same result, while for K=3 runs result in two different solutions represented here. D. Observed heterozygosity per sample vs. depth of coverage of the sample. Shading represents the confidence interval around the regression line. Differences in diversity among the ancient samples might be attributed to differences in coverage, as the one with higher coverage shows similar heterozygosity to other ancient samples when subsampled to a similar depth of coverage (2.58x, 3.15 e-6; Table S4), but differences between ancient and modern samples cannot be explained only by differences in coverage.

Fig. 2. A. Genetic diversity (nucleotide diversity, π, left panel; Watterson's theta, θ_W, right panel) in different genomic features for contemporary (Doñana, and Andújar) and ancient populations. UTR = untranslated regions, CDS = coding sequence, lnc = long-non-coding, nc = non-coding, and UCNE = ultra-conserved-non-coding-elements. Bars on contemporary points represent standard deviation calculated over 10kb windows using 100 iterations. B. Percentage of CDS in genomic windows with lowest diversity difference (outliers) compared to the rest of windows. Outlier windows were defined as those showing extreme diversity difference between ancient and contemporary samples (i.e. ancient diversity minus contemporary diversity) lower than the average minus 2*standard deviation. Comparisons include ancient vs. current Doñana and ancient vs. current Andujar, and both π, and θ_W. Diamonds represent the mean value and lines represent median.

Fig. 3. Results of D statistics tests. *EL* = Eurasian lynx, *IL* = Iberian lynx. Western EL included genomes sampled in Kirov, Caucasus, Balkans, and Carpathians, while Eastern EL genomes were sampled in Primorsky-Krai, and Yakutia. Red and white points show significant (absolute Z score > 3) and non-significant (absolute Z score < 3) D values, respectively. The five different tree topologies tested (A-E) are displayed for each category of D values shown, with double headed arrows indicating the admixing lineages supported by significant tests.

Fig. 4. $\hat{f}$ tests on a five taxon topology (((ancient Iberian lynx, contemporary Iberian lynx), (western Eurasian lynx, western Eurasian lynx), outgroup) to estimate the genomic fraction of Eurasian lynx introgression in contemporary Iberian lynx above that occurring in ancient Iberian lynx, assuming unidirectional gene flow (schematic shown to right). Each sampled contemporary Iberian lynx is indicated on the x axis, with clouds of points showing results generated using different combinations of the other 3 ingroup individuals. Points corresponding to the three sampled ancient lynx are indicated by different colours: red (Algarve, 2 kya), blue (Catalonia, 2.5 kya) and yellow (Andujar, 4.2 kya), respectively. Western Eurasian lynx (Kirov, Caucasus, Balkans, and Carpathians) were used in these tests since, based on geographic proximity to the Iberian lynx, they are likely to best represent the introgressing population. All comparisons provided a statistically significant (absolute Z score > 3) signal of higher admixture in modern than in ancient lynx.

SUPPLEMENTARY FIGURES

Fig. S1. Authentication of ancient DNA data using MapDamage. On the left, cytosine deamination patterns. X axis indicates the relative nucleotide position of the reads. Plots show the proportion of T where the reference genome possesses a C (red) and proportion of A where the reference possesses a G (blue). Increased C to T substitutions towards the ends of the read are typical damage patterns for ancient data, although the single-stranded library preparation with UDG (uracil-DNA glycosylase) treatment reduced this pattern. Plot on the right represents the fragment length distribution. Minimum read length for mapping used was 30 bp, resulting in a truncation of the plot.

Fig. S2. Alternative clustering patterns obtained in 5 runs of NGSadmix for K=4 and K=5. Population names on top, with number of samples within parentheses.

Fig. S3. Diversity of the ancient population (n=3), and different random subsamples (n=3) of individuals from the contemporary populations, Andújar and Doñana, considering both transitions and transversions (A) and transversion only (B). Although not always visible, bars represent the standard deviation obtained after bootstrapping over windows.

Fig. S4. Relative difference in nucleotide diversity (A) or Watterson's estimator (B) between ancient and contemporary samples in features selected to represent neutral (intergenic, introns) or selected (CDS, UCNE) features. The relative difference was calculated as (contemporary diversity - ancient diversity) / (contemporary diversity + ancient diversity), as in Lucena-Perez et al. (2021).

Fig. S5. Results of D statistics tests. On the left, the different tree topologies tested (A-G). *EL* = Eurasian lynx, *IL* = Iberian lynx. Western EL included genomes sampled in Kirov, Caucasus, Balkans, and Carpathians, while Eastern EL genomes were sampled in Primorsky-Krai, and Yakutia. All topologies were tested using the domestic cat as the outgroup. Red and white points show significant (absolute Z score > 3) and non-significant (absolute Z score < 3) D values, respectively. The seven different tree topologies tested (A-G) are displayed for each category of D values shown, with double headed arrows indicating the admixing lineages supported by significant tests. A, shows similar introgression in different contemporary IL individuals. B and C show similar and non-significant D statistic when different eastern and western Eurasian lynx individuals are compared. D and E show higher admixture signal from contemporary Eurasian lynx than from a single ancient Eurasian lynx from the Iberian Peninsula, whereas ancient Iberian lynx is less admixed with ancient EL than contemporary Western EL (F) and similarly than Eastern EL (G).

Fig. S6. Results of phylogenetic tests of gene flow direction. The schematic at the top of the figure shows topologies informative on gene flow from Eurasian into Iberian lynx. An excess of genomic

windows returning topologies where the less-admixed ancient Iberian lynx is in a basal position relative to the number of genomic windows retuning topologies where the more-admixed modern Iberian lynx is basal indicate gene flow from Eurasian lynx onto the modern Iberian lynx lineage, above that occurring into the ancient Iberian lynx lineage. The lower part of the figure shows individual results (points) generated using each combination of one modern Iberian lynx (30 individuals total), the ancient Iberian lynx from Catalonia (2,520 ± 30 BP), and one of the two Eurasian lynx as representing each of the main Eurasian clades. Arrows indicate the more frequently observed topology at each side of the axis, with the central point (equal ratio) indicating an absence of received gene flow. Note the arrow position is not an indication of the timing of gene flow, and is included to aid interpretation of the figure. An excess (mean 1.84-fold higher) of topologies with the less-admixed ancient Iberian lynx in the basal position in all comparisons indicates that the admixture inferred using D statistics can be attributed, at least in part, to gene flow from Eurasian lynx into ancestors of contemporary Eurasian lynx.

Acknowledgements

This research was funded by the Spanish Dirección General de Investigación Científica y Técnica, through projects CGL2013-47755-P and CGL2017-84641-P to J.A.G and is an extension of a project on ancient lynx genetics granted to Miguel Delibes de Castro by the Fundación BBVA. M.L.P. was supported by a PhD contract from Programa Internacional de Becas “La Caixa-Severo Ochoa.” J.N. received financial support through projects HAR2014- 55131 from the Ministerio de Ciencia e Innovación (MICINN) and SGR2014-108 from Generalitat de Catalunya. We acknowledge support from Science for Life Laboratory, the Knut and Alice Wallenberg Foundation, the National Genomics Infrastructure funded by the Swedish Research Council, and Uppsala Multidisciplinary Center for Advanced Computational Science for assistance with massively parallel sequencing and access to the UPPMAX computational infrastructure. We also acknowledge the support of the Supercomputing Wales project, which is part-funded by the European Regional

Development Fund (ERDF) via Welsh Government. Logistical support was provided by the Laboratorio de Ecología Molecular (LEM-EBD) certified to ISO9001:2015 and ISO14001:2015 quality and environmental management systems. Data processing and most calculations and analyses were carried out in the Genomics servers of Doñana's Singular Scientific-Technical Infrastructure (ICTS-RBD), with additional computing and storage resources provided by Fundación Pública Galega, Centro Tecnolóxico de Supercomputación de Galicia (CESGA). Logistical laboratory support was provided by the Laboratorio de Ecología Molecular (LEM-EBD) certified to ISO9001:2015 and ISO14001:2015 quality and environmental management systems. Data processing and most calculations and analyses were carried out in the Genomics servers of Doñana's Singular Scientific-Technical Infrastructure (ICTS-RBD), with additional computing and storage resources provided by Fundación Pública Galega Centro Tecnolóxico de Supercomputación de Galicia (CESGA).

AUTHOR CONTRIBUTION

J.A.G. conceived the project, A.B., J.A.G. and M.L.P., designed the study; C.D., F.N., and J.N. provided ancient samples and critical input on archeological context; M.L.P. performed the lab work under J.L.A.P. and M.H. supervision; A.B., J.L.A.P., M.L.P., analysed data; A.B., J.A.G., J.L.A.P., and M.L.P. interpreted the results, with critical input by M.H. and L.D.; M.L.P. drafted the manuscript with support from A.B. and J.A.G. and input by J.L.A.P., C.D., J.N., M.H. and L.D.. All authors approved the final version of the manuscript.

Data Availability

Merged reads sequence data is available for download at ENA repository under study number PRJEB58855.

References

Abascal F, Corvelo A, Cruz F, *et al.* (2016) Extreme genomic erosion after recurrent demographic bottlenecks in the highly endangered Iberian lynx. *Genome Biology* **17**, 251.

Allendorf FW, Funk WC, N. Aitken S, Byrne M, Luikart G (2021) *Conservation and the genomics of populations*, 3. edn. Oxford University Press, New York.

Barlow A, Cahill JA, Hartmann S, *et al.* (2018) Partial genomic survival of cave bears in living brown bears. *Nature Ecology & Evolution* **2**, 1563-1570.

Barlow A, Hartmann S, González J, Hofreiter M, Paijmans J (2020) Consensify: A Method for Generating Pseudohaploid Genome Sequences from Palaeogenomic Datasets with Reduced Error Rates. *Genes* **11**, 50.

Bazzicalupo E, Lucena-Perez M, Kleinman-Ruiz D, *et al.* (2022) History, demography and genetic status of Balkan and Caucasian Lynx lynx (Linnaeus, 1758) populations revealed by genome-wide variation. *Diversity and Distributions* **28**, 65-82.

Bell DA, Robinson ZL, Funk WC, *et al.* (2019) The Exciting Potential and Remaining Uncertainties of Genetic Rescue. *Trends in Ecology & Evolution* **34**, 1070-1079.

Borg I, Groenen PJF (1997) *Modern multidimensional scaling: theory and applications* Springer, New York.

Brink FHVD (1970) Distribution and speciation of some Carnivores. *Mammal Review* **1**, 67-79.

Buckley R, Davis B, Brashear W, *et al.* (2020) A new domestic cat genome assembly based on long sequence reads empowers feline genomic medicine and identifies a novel gene for dwarfism. *PLoS Genetics* **16**, e1008926.

Canty A, Ripley B (2014) boot: Bootstrap R (S-Plus) Functions. R package version 1.3-11.

Casas-Marcé M, Marmesat E, Soriano L, *et al.* (2017) Spatio-temporal dynamics of genetic variation in the Iberian lynx along its path to extinction reconstructed with ancient DNA. *Molecular Biology and Evolution* **34**, 2893–2907.

Chan WY, Hoffmann AA, van Oppen MJH (2019) Hybridization as a conservation management tool. *Conservation Letters* **12**.

Clavero M, Delibes M (2013) Using historical accounts to set conservation baselines: the case of lynx species in Spain. *Biodiversity and Conservation* **22**, 1691-1702.

Corbet GB, Hill JE (1986) *A world list of mammalian species*, 2nd edn. British Museum of Natural History, London.

D'Elia J, Haig SM, Mullins TD, Miller MP (2016) Ancient DNA reveals substantial genetic diversity in the California Condor (Gymnogyps californianus) prior to a population bottleneck. *Condor* **118**, 703-714.

Dabney J, Knapp M, Glocke I, *et al.* (2013) Complete mitochondrial genome sequence of a Middle Pleistocene cave bear reconstructed from ultrashort DNA fragments. *Proceedings of the National Academy of Sciences*.

Dabney J, Meyer M (2012) Length and GC-biases during sequencing library amplification: A comparison of various polymerase-buffer systems with ancient and modern DNA sequencing libraries. *BioTechniques* **52**, 87-94.

de Bruyn M, Hoelzel AR, Carvalho GR, Hofreiter M (2011) Faunal histories from Holocene ancient DNA. *Trends in Ecology & Evolution* **26**, 405-413.

Diez-del-Molino D, Sanchez-Barreiro F, Barnes I, Gilbert MTP, Dalen L (2018) Quantifying Temporal Genomic Erosion in Endangered Species. *Trends in Ecology & Evolution* **33**, 176-185.

Dufresnes C, Miquel C, Remollino N, *et al.* (2018) Howling from the past: historical phylogeography and diversity losses in European grey wolves. *Proceedings of the Royal Society B-Biological Sciences* **285**.

Durand EY, Patterson N, Reich D, Slatkin M (2011) Testing for Ancient Admixture between Closely Related Populations. *Molecular Biology and Evolution* **28**, 2239-2252.

Dussex N, von Seth J, Robertson BC, Dalen L (2018) Full Mitogenomes in the Critically Endangered Kakapo Reveal Major Post-Glacial and Anthropogenic Effects on Neutral Genetic Diversity. *Genes* **9**.

Evanno G, Regnaut S, Goudet J (2005) Detecting the number of clusters of individuals using the software STRUCTURE: a simulation study. *Molecular Ecology* **14**, 2611-2620.

Feng S, Fang Q, Barnett R, *et al.* (2019) The Genomic Footprints of the Fall and Recovery of the Crested Ibis. *Current Biology* **29**, 340-349.e347.

Frankham R, Ballou JD, Briscoe DA (2010) *Introduction to conservation genetics*, 2nd ed edn. Cambridge University Press, Cambridge ; New York.

Fulton TL (2012) Setting Up an Ancient DNA Laboratory. In: *Ancient DNA: Methods and Protocols* (eds. Shapiro B, Hofreiter M), pp. 1-11. Humana Press, New York.

Fumagalli M (2013) Assessing the Effect of Sequencing Depth and Sample Size in Population Genetics Inferences. *Plos One* **8**.

Fumagalli M, Vieira FG, Linderoth T, Nielsen R (2014) ngsTools: methods for population genetics analyses from next-generation sequencing data. *Bioinformatics* **30**, 1486-1487.

Gansauge MT, Meyer M (2013) Single-stranded DNA library preparation for the sequencing of ancient or damaged DNA. *Nature Protocols* **8**, 737-748.

Green RE, Krause J, Briggs AW, *et al.* (2010) A Draft Sequence of the Neandertal Genome. *Science* **328**, 710-722.

Gunther T, Nettelblad C (2019) The presence and impact of reference bias on population genomic studies of prehistoric human populations. *PLoS Genetics* **15**.

Harris A, Foley N, Williams T, Murphy W (2022) Tree House Explorer: A Novel Genome Browser for Phylogenomics. Molecular Biology and Evolution 39, msac130.

Hofreiter M, Barnes I (2010) Diversity lost: are all Holarctic large mammal species just relict populations? *BMC Biology* **8**.

Iacolina L, Corlatti L, Buzan E, Safner T, Sprem N (2019) Hybridisation in European ungulates: an overview of the current status, causes, and consequences. *Mammal Review* **49**, 45-59.

Jiménez J, Clavero M, Reig-Ferrer A (2018) New old news on the “Lobo cerval” (Lynx lynx?) in NE Spain. *Galemys, Spanish Journal of Mammalogy* **30**, 1-6.

Jónsson H, Ginolhac A, Schubert M, Johnson PLF, Orlando L (2013) mapDamage2.0: fast approximate Bayesian estimates of ancient DNA damage parameters. *Bioinformatics* **29**, 1682-1684.

Kim SY, Lohmueller KE, Albrechtsen A, *et al.* (2011) Estimation of allele frequency and association mapping using next-generation sequencing data. *BMC Bioinformatics* **12**.

Kleinman-Ruiz D, Lucena-Perez M, Villanueva B, *et al.* (2022) Purging of deleterious burden in the endangered Iberian lynx. *Proceedings of the National Academy of Sciences* **119**, e2110614119.

Kopelman NM, Mayzel J, Jakobsson M, Rosenberg NA, Mayrose I (2015) Clumpak: a program for identifying clustering modes and packaging population structure inferences across K. *Molecular Ecology Resources* **15**, 1179-1191.

Korlević P, Gerber T, Gansauge M-T, *et al.* (2015) Reducing microbial and human contamination in DNA extractions from ancient bones and teeth. *BioTechniques* **59**, 87-93.

Korneliussen TS, Albrechtsen A, Nielsen R (2014) ANGSD: Analysis of Next Generation Sequencing Data. *BMC Bioinformatics* **15**.

Korneliussen TS, Moltke I, Albrechtsen A, Nielsen R (2013) Calculation of Tajima's D and other neutrality test statistics from low depth next-generation sequencing data. *BMC Bioinformatics* **14**.

Kumar V, Lammers F, Bidon T, *et al.* (2017) The evolutionary history of bears is characterized by gene flow across species. *Scientific Reports* **7**.

Kurten B, Granqvist E (1987) Fossil Pardel Lynx (Lynx-Pardina-Spelaea Boule) from a Cave in Southern France. *Annales Zoologici Fennici* **24**, 39-43.

Leigh DM, Hendry AP, Vázquez-Domínguez E, Friesen VL (2019) Estimated six per cent loss of genetic variation in wild populations since the industrial revolution. *Evolutionary Applications* **12**, 1505-1512.

Li G, Davis BW, Eizirik E, Murphy WJ (2016) Phylogenomic evidence for ancient hybridization in the genomes of living cats (Felidae). *Genome Research* **26**, 1-11.

Li G, Figueiró HV, Eizirik E, Murphy WJ (2019) Recombination-aware phylogenomics reveals the structured genomic landscape of hybridizing cat species. *Molecular Biology and Evolution* **36**, 2111-2126.

Li H (2011) A statistical framework for SNP calling, mutation discovery, association mapping and population genetical parameter estimation from sequencing data. *Bioinformatics* **27**, 2987-2993.

Li H, Durbin R (2009) Fast and accurate short read alignment with Burrows–Wheeler transform. *Bioinformatics* **25**, 1754-1760.

Li H, Handsaker B, Wysoker A, *et al.* (2009) The Sequence Alignment/Map format and SAMtools. *Bioinformatics* **25**, 2078-2079.

Lucena-Perez M, Bazzicalupo E, Paijmans J, *et al.* (2022) Ancient genome provides insights into the history of Eurasian lynx in Iberia and Western Europe. *Quaternary Science Reviews* **285**, 107518.

Lucena-Perez M, Kleinman-Ruiz D, Marmesat E, *et al.* (2021) Bottleneck-associated changes in the genomic landscape of genetic diversity in wild lynx populations. *Evolutionary Applications* **14**, 2664-2679.

Lucena-Perez M, Marmesat E, Kleinman-Ruiz D, *et al.* (2020) Genomic patterns in the widespread Eurasian lynx shaped by Late Quaternary climatic fluctuations and anthropogenic impacts. *Molecular Ecology* **29**, 812-828.

Martin AD, Quinn KM, Park JH (2011) MCMCpack: Markov Chain Monte Carlo in R. *Journal of Statistical Software* **42**, 1 - 21.

Matjuschkin EN (1978) *Der Luchs. Wittenberg Lutherstadt, A. Ziemsen Verlag, 160 pp* Wittenberg Lutherstadt, A. Ziemsen Verlag.

McKenna A, Hanna M, Banks E, *et al.* (2010) The Genome Analysis Toolkit: A MapReduce framework for analyzing next-generation DNA sequencing data. *Genome Research* **20**, 1297-1303.

Mecozzi B, Sardella R, Boscaini A, *et al.* (2021) The tale of a short-tailed cat: New outstanding Late Pleistocene fossils of Lynx pardinus from southern Italy. *Quaternary Science Reviews* **262**.

Page AJ, Taylor B, Delaney AJ, *et al.* (2016) SNP-sites: rapid efficient extraction of SNPs from multi-FASTA alignments. *Microb Genom* **2**, e000056.

Palkopoulou E, Lipson M, Mallick S, *et al.* (2018) A comprehensive genomic history of extinct and living elephants. *Proceedings of the National Academy of Sciences of the United States of America* **115**, E2566-E2574.

Pease, J. B., & Hahn, M. W. (2015) Detection and Polarization of Introgression in a Five-Taxon Phylogeny. Systematic Biology, 64(4), 651-662.

Quilodrán CS, Montoya-Burgos JI, Currat M (2020) Harmonizing hybridization dissonance in conservation. *Commun Biol* **3**, 391.

R_Core_Team (2019) R: A Language and Environment for Statistical Computing. R Foundation for Statistical Computing, Vienna, Austria.

Ralls K, Ballou JD, Dudash MR, *et al.* (2018) Call for a Paradigm Shift in the Genetic Management of Fragmented Populations. *Conservation Letters* **11**, n/a-n/a.

Rodríguez-Varela R, García N, Nores C, *et al.* (2016) Ancient DNA reveals past existence of Eurasian lynx in Spain. *Journal of Zoology* **298**, 94-102.

Rodríguez-Varela R, Tagliacozzo A, Ureña I, *et al.* (2015) Ancient DNA evidence of Iberian lynx palaeoendemism. *Quaternary Science Reviews* **112**, 172-180.

Sánchez-Barreiro F, Gopalakrishnan S, Ramos-Madrigal J, *et al.* (2021) Historical population declines prompted significant genomic erosion in the northern and southern white rhinoceros (Ceratotherium simum). *Molecular Ecology* **30**, 6355-6369.

Sheng G-L, Basler N, Ji X-P, *et al.* (2019) Paleogenome Reveals Genetic Contribution of Extinct Giant Panda to Extant Populations. *Current Biology*.

Sheng GL, Barlow A, Cooper A, *et al.* (2018) Ancient DNA from Giant Panda (Ailuropoda melanoleuca) of South-Western China Reveals Genetic Diversity Loss during the Holocene. *Genes* **9**.

Skotte L, Korneliussen TS, Albrechtsen A (2013) Estimating Individual Admixture Proportions from Next Generation Sequencing Data. *Genetics* **195**, 693-+.

Stamatakis A (2006) RAxML-VI-HPC: Maximum likelihood-based phylogenetic analyses with thousands of taxa and mixed models. *Bioinformatics* **22**, 2688-2690.

Tallmon Da, Luikart G, Waples RS (2004) The alluring simplicity and complex reality of genetic rescue. *Trends in Ecology & Evolution* **19**, 489-496.

Tumlison R (1987) *Felis lynx*. *Mammalian Species* **269**, 1-8.

van der Valk T, Diez-del-Molino D, Marques-Bonet T, Guschanski K, Dalen L (2019) Historical Genomes Reveal the Genomic Consequences of Recent Population Decline in Eastern Gorillas. *Current Biology* **29**, 165-+.

Vila C, Sundqvist AK, Flagstad O, *et al.* (2003) Rescue of a severely bottlenecked wolf (Canis lupus) population by a single immigrant. *Proceedings of the Royal Society of London Series B-Biological Sciences* **270**, 91-97.

Weigel I (1961) *Das Fellmuster der wildlebenden Katzenarten und der Hauskatze in vergleichender und stammesgeschichtlicher Hinsicht* Säugetierkundliche Mitteilungen, München.

Werdelin L (1981) The evolution of lynxes. *Ann Zool Fennici* **18**, 37-71.

Whiteley AR, Fitzpatrick SW, Funk WC, Tallmon DA (2015) Genetic rescue to the rescue. *Trends in Ecology & Evolution* **30**, 42-49.

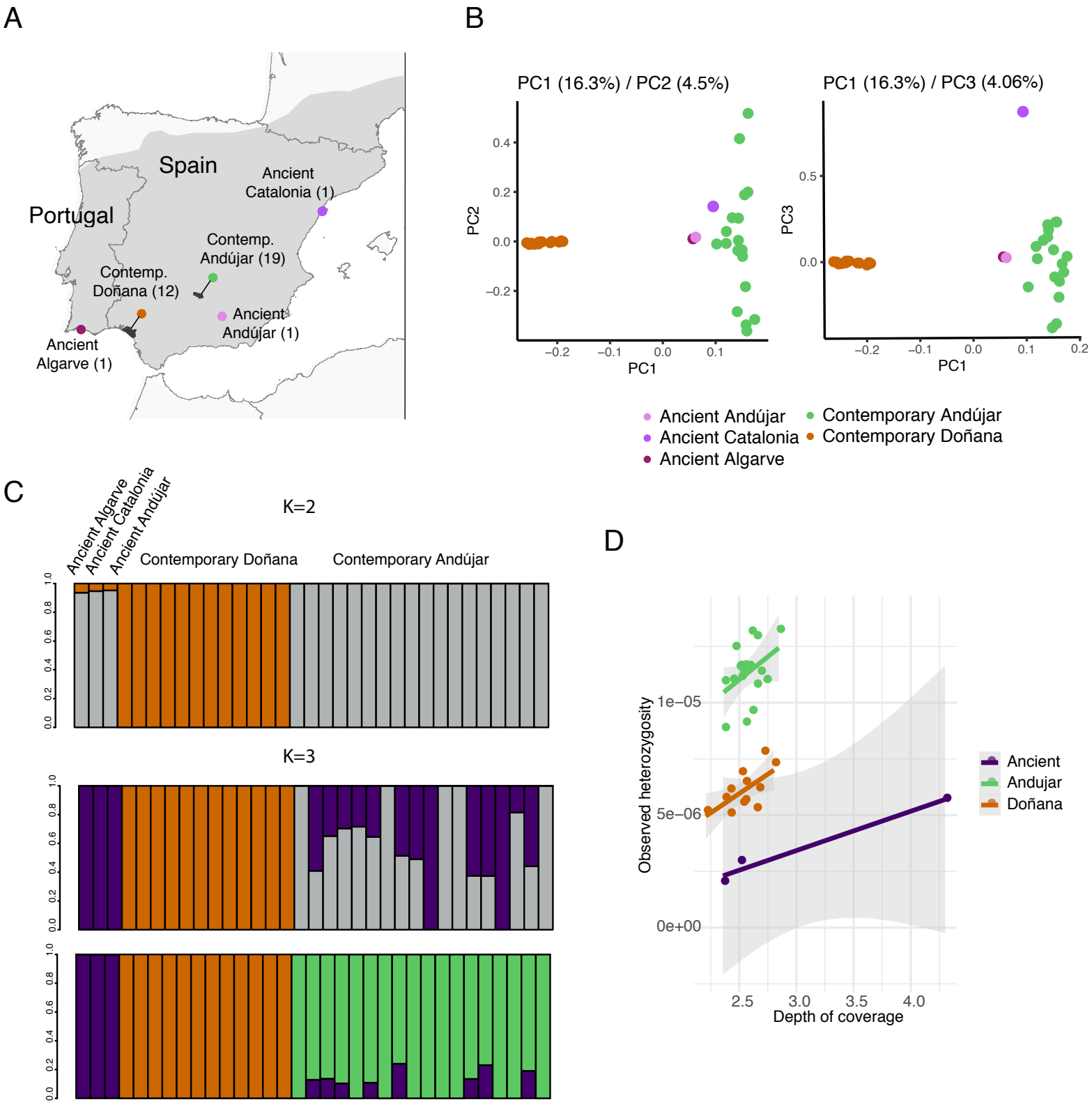
A
Spain
Portugal
Ancient Catalonia (1)
Contemp. Andújar (19)
Contemp. Doñana (12)
Ancient Andújar (1)
Ancient Algarve (1)
B
PC1 (16.3%) / PC2 (4.5%)
PC1 (16.3%) / PC3 (4.06%)
PC1
PC2
PC3
Ancient Andújar
Ancient Catalonia
Ancient Algarve
Contemporary Andújar
Contemporary Doñana
C
K=2
K=3
Ancient Algarve
Ancient Catalonia
Ancient Andújar
Contemporary Doñana
Contemporary Andújar
D
Observed heterozygosity
Depth of coverage
Ancient
Andujar
Doñana

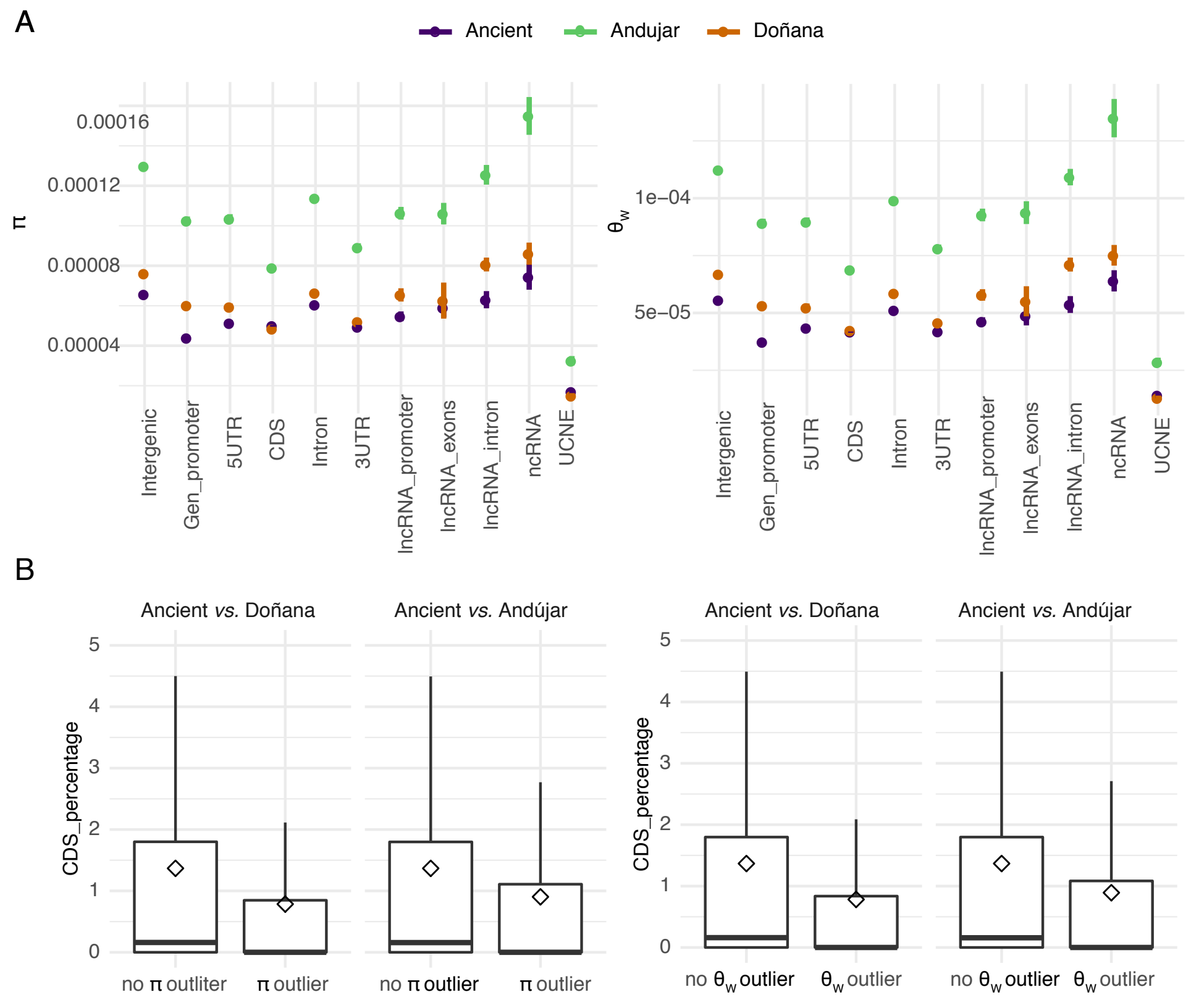
A
Ancient
Andujar
Doñana
π
0.00016
0.00012
0.00008
0.00004
θw
1e−04
5e−05
Intergenic
Gen_promoter
5UTR
CDS
Intron
3UTR
lncRNA_promoter
lncRNA_exons
lncRNA_intron
ncRNA
UCNE
B
Ancient vs. Doñana
Ancient vs. Andújar
CDS_percentage
no π outliter
π outlier
no θw outlier
θw outlier

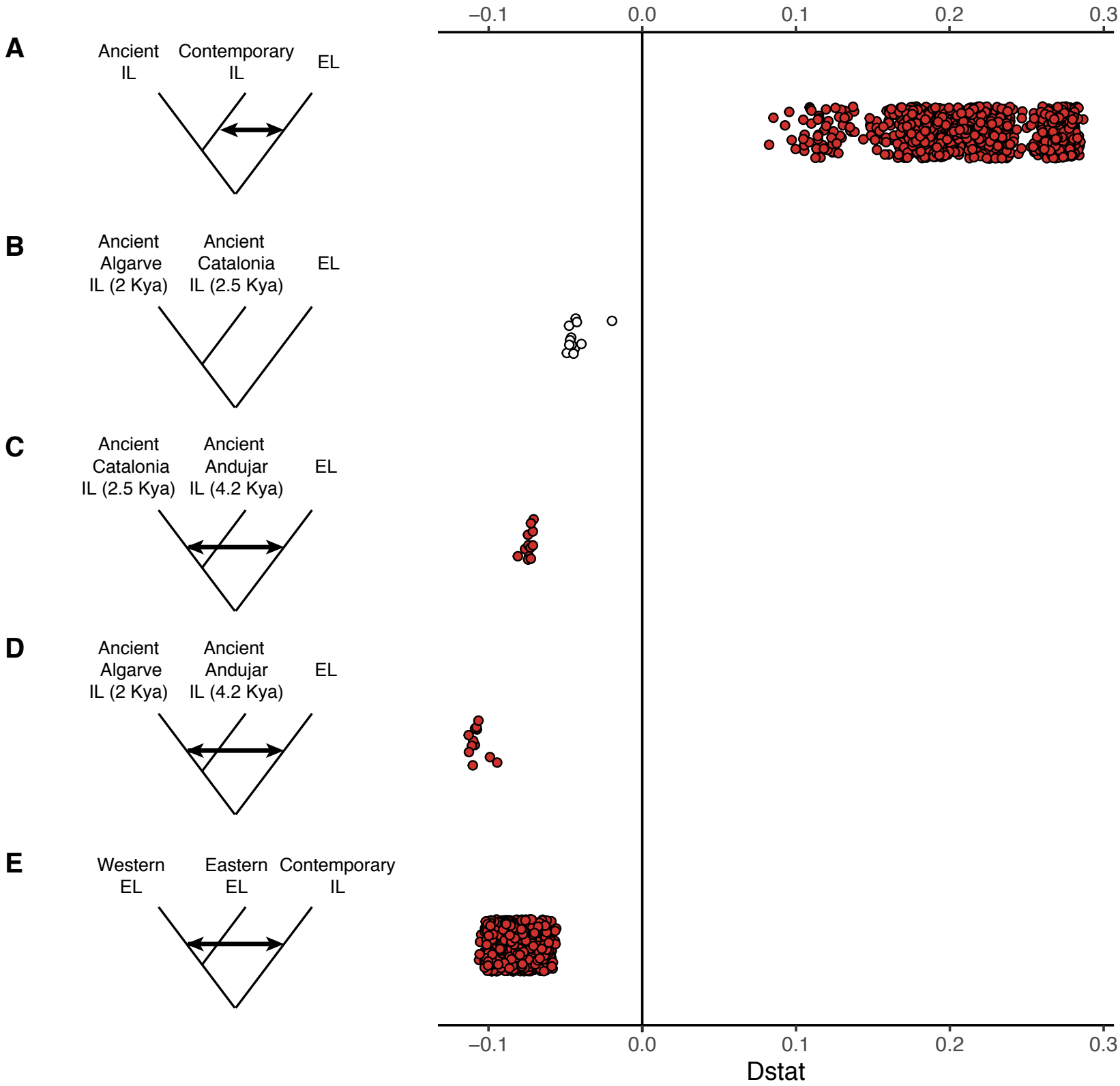
A
Ancient IL
Contemporary IL
EL
B
Ancient Algarve IL (2 Kya)
Ancient Catalonia IL (2.5 Kya)
EL
C
Ancient Catalonia IL (2.5 Kya)
Ancient Andujar IL (4.2 Kya)
EL
D
Ancient Algarve IL (2 Kya)
Ancient Andujar IL (4.2 Kya)
EL
E
Western EL
Eastern EL
Contemporary IL
−0.1
0.0
0.1
0.2
0.3
Dstat

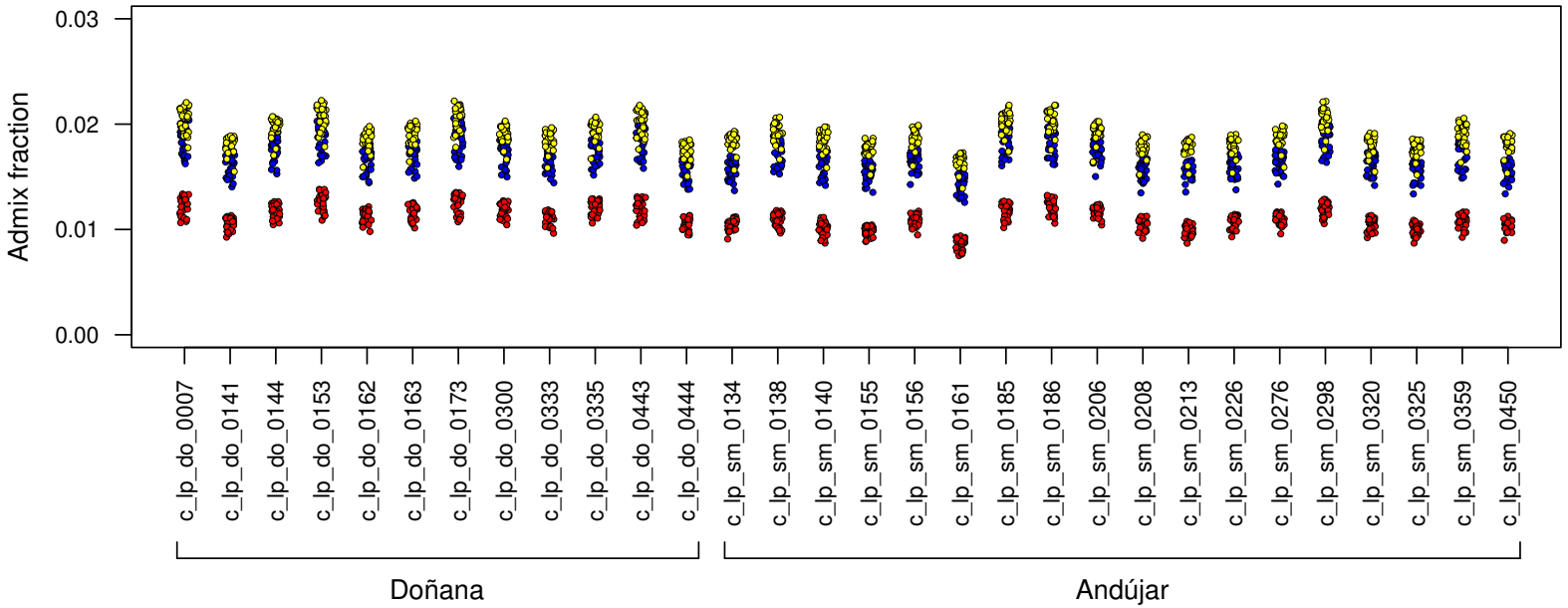
Admix fraction
0.03
0.02
0.01
0.00
c_lp_do_0007
c_lp_do_0141
c_lp_do_0144
c_lp_do_0153
c_lp_do_0162
c_lp_do_0163
c_lp_do_0173
c_lp_do_0300
c_lp_do_0333
c_lp_do_0335
c_lp_do_0443
c_lp_do_0444
c_lp_sm_0134
c_lp_sm_0138
c_lp_sm_0140
c_lp_sm_0155
c_lp_sm_0156
c_lp_sm_0161
c_lp_sm_0185
c_lp_sm_0186
c_lp_sm_0206
c_lp_sm_0208
c_lp_sm_0213
c_lp_sm_0226
c_lp_sm_0276
c_lp_sm_0298
c_lp_sm_0320
c_lp_sm_0325
c_lp_sm_0359
c_lp_sm_0450
Doñana
Andújar

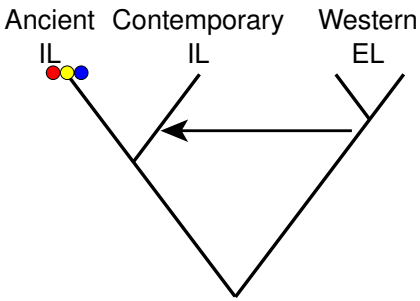
Ancient
IL
Contemporary
IL
Western
EL